PHYSICAL REVIEW LETTERS

Polarization-Reversal-Induced Damping of Left-Hand Polarized Wave on Electron Cyclotron Resonance

K. Takahashi,* T. Kaneko, and R. Hatakeyama

Department of Electronic Engineering, Tohoku University, Sendai, 980-8579, Japan

The left-hand polarized wave, which has been believed not to be related to electron cyclotron resonance (ECR), is for the first time demonstrated to be damped near the ECR point in an inhomogeneously magnetized plasma as a result of the polarization reversal to the right-hand polarized wave. The polarization reversal is found to be caused by the existence of the boundary between a plasma and a vacuum region, the local point of which shifts depending on the plasma column radius. This phenomenon is quantitatively explained in terms of the dispersion relation including the effect of the radial boundary condition.

Electromagnetic waves in magnetized plasmas are important plasma waves quoted and utilized in thermonuclear fusion and plasma processing researches. Especially, much attention has been focused on the waves in the range of electron cyclotron resonance (ECR) frequency. It was reported in the field of thermonuclear fusion that ECR is effective in the formation of local-confining potential [1,2], electron cyclotron current drive [3], suppression of disruption in a tokamak [4], and so on. In the field of processing plasma, on the other hand, it was reported that ECR is useful for the production of plasmas with high density, large diameter, and uniformity [5,6].

Propagation and absorption of high frequency electromagnetic waves in plasmas have basically been significant research subjects since they play important roles in pursuing the above-mentioned applications. A right-hand polarized wave (RHPW) is straightforwardly accepted to be absorbed near the ECR point and its associated investigations have been performed for a long time [7,8], while a left-hand polarized wave (LHPW) was believed not to be related to ECR. In recent laboratory experimental results, however, the LHPW was reported to be dissipated near the ECR point in ECR discharges [9], just like the RHPW. In laboratory plasmas electromagnetic waves are generally affected by boundaries between a plasma and a vacuum region, and at a conducting vacuum wall. In order to explain the unexpected dissipation of the LHPW, the polarization reversal from the LHPW to the RHPW in bounded plasmas is theoretically suggested for the case of $m = -1$ mode [10], where m is an azimuthal mode number. This theory, however, focuses upon only the effect of radial variations and does not emphasize a more dominant effect of axial profiles in the polarization reversal process. Besides, the experiment neither clarifies detailed effects of the boundaries nor gives any evidence of the polarization reversal. This is because the waves in the ECR frequency range are simultaneously utilized both for producing plasmas by the ECR discharge and for studying wave propagations, making it difficult to obtain clear-cut

experimental results. Therefore, we have claimed that it is necessary to perform the measurements of propagation and absorption of small amplitude microwaves in a steady-state plasma produced by a direct current discharge. According to preliminary measurements, the damping region of the LHPW appears to be more local than that of the RHPW [11], the phenomenon of which is supposed to be due to the polarization reversal, and can be applicable to more localized electron heating and potential-structure control. In addition, it is generally important to understand the damping mechanisms of the electromagnetic wave since the absorption of the wave dominates the density profile of the produced plasma, which is often required to be controlled in various kind of plasma physics and application experiments. Therefore, the purpose of the present work is to clarify the damping mechanisms of the LHPW near the ECR point from the viewpoint of the polarization reversal from the LHPW to the RHPW, and to solve the detailed effects of the boundaries on the wave propagation and absorption. In this Letter, it is directly demonstrated for the first time that the polarization reversal from the LHPW to the RHPW occurs in the process of axial propagation and is caused by an existence of the radial boundary condition.

Experiments are performed in the Q_T-Upgrade machine of Tohoku University as shown in Fig. 1, which has a cylindrical vacuum chamber about 450 cm in length and 20.8 cm in diameter. A coaxial bounded plasma is produced by a direct current discharge between an oxide cathode and a tungsten mesh anode with a limiter in low pressure argon gas (90 mPa). The formation of a clear boundary between the plasma and the vacuum region is realized by using the limiter, which also can control the plasma radius r_p in the range of 2.5–4 cm. The plasma column is terminated on a glass end plate located at the opposite end of the plasma source. Under these conditions, the electron density and temperature are $n_e \simeq 9 \times 10^{10}$ cm^{-3} and $T_e \simeq 3$ eV, respectively. Magnetic-field configurations are inhomogeneous as presented in Fig. 1, where a characteristic length L_B of magnetic-field gradient
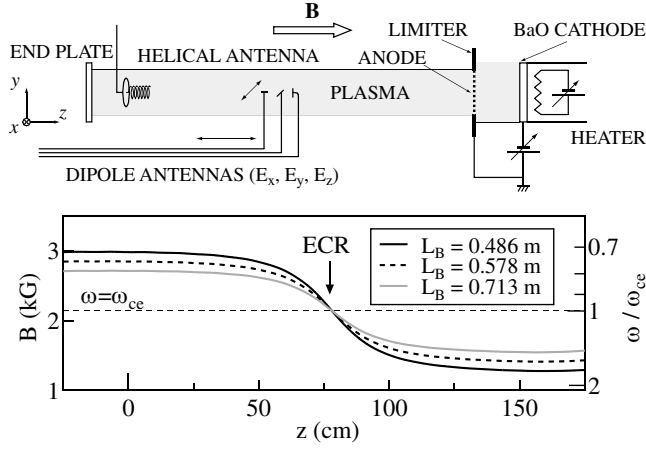
215001-1

FIG. 1. Schematic of experimental setup and external magnetic-field configuration. The microwave frequency is $\omega/2\pi = 6$ GHz.

is defined as $L_B = [(1/B)dB/dz]^{-1}$ and the condition of $\omega_{pe} < \omega_{ce}$ is satisfied in the plasma column ($\omega_{pe}/2\pi$: electron plasma frequency, $\omega_{ce}/2\pi$: electron cyclotron frequency).

A microwave (frequency $\omega/2\pi = 6$ GHz, power 150 mW) is selectively launched in the high magnetic-field region as the LHPW by a helical antenna ($z = 0$ cm) [11]. The wave propagates toward the ECR point ($z = 78$ cm) satisfying the condition of $\omega/\omega_{ce} < 1$. The wave patterns are obtained with an interference method through axially and radially movable balanced dipole antennas, which can receive each component of electric fields of the wave, i.e., E_x, E_y, and E_z.

Figure 2(a) shows the typical interferometric wave patterns of E_x (solid line) and E_y (dashed line) at the radial center of the plasma column for $L_B = 0.629$ m and $r_p = 3$ cm. The wave patterns disclose the unexpected damping of the wave near the ECR point in spite of the selective launch of the LHPW. The long (LW) and short (SW) wavelength components decomposed from the observed wave pattern in Fig. 2(a) are presented in Fig. 2(b). Here, the digital high- and low-pass filters with the border at $k_{\parallel}/2\pi = 0.2$ cm^{-1}, which corresponds to the wave number of 6 GHz microwave in vacuum, are used. It is noticed that the LW damps and the SW grows around $z = 60$ cm in Fig. 2(b). Moreover, it is obviously observed that the phase difference of E_x to E_y for the LW and the SW is oppositely shifted. Therefore, we plot the axial profiles of the electric-field vector of the LW and the SW in Figs. 3(a) and 3(b), respectively, which are obtained from the wave patterns of E_x and E_y. Figure 3 signifies that the polarization of the SW is opposite to that of the LW. As the wave propagates toward the plasma source, it is identified that the polarization of the LW and the SW are left- and right-handed, respectively.

The results in Figs. 2 and 3, i.e., damping of the LW (LHPW) and growth of the SW (RHPW), are the first
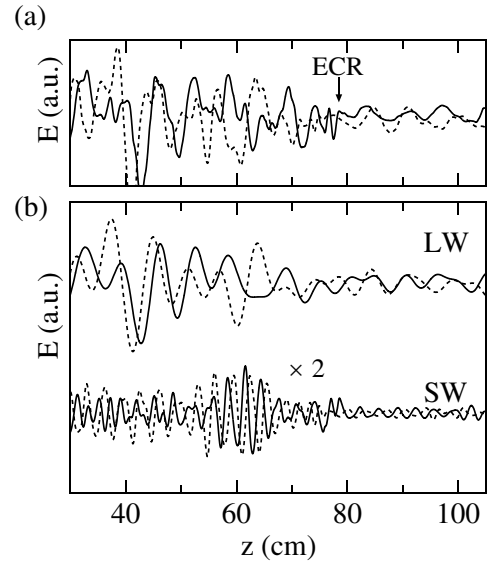

FIG. 2. (a) Interferometric wave pattern of E_x (solid line) and E_y (dashed line) for $L_B = 0.629$ m and $r_p = 3$ cm. (b) LW and SW components included in the wave pattern of (a).

experimental demonstrations of the polarization reversal from the LHPW to the RHPW near the ECR point. As a result, the launched LHPW is found to be absorbed near the ECR point through the polarization reversal. Here, accord-
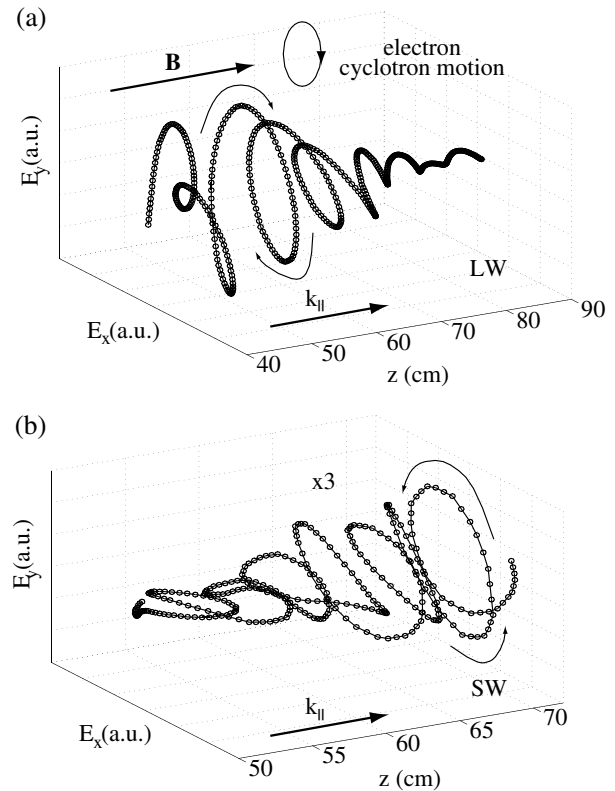

FIG. 3. Axial profiles of the electric-field vector of (a) the LW and (b) the SW in transverse plane against the magnetic-field lines.

ing to the comparison of the experimental amplitudes with the theoretical electric-field strengths given by the energy flux conservation, we mention that the appearance of the RHPW around $z \simeq 60$ cm is considered to have no relation with the reduction of the group velocity in a dispersion relation described later.

For the purpose of understanding the mechanism of the polarization reversal in detail, the RHPW components decomposed from the observed wave patterns for $L_B = 0.486$, 0.578, and 0.713 m are presented in Fig. 4(a) for the case of $r_p = 3$ cm. In order to estimate the polarization reversal point, we define z_{pr} as the axial point where the RHPW has a maximum amplitude as indicated by arrows in Fig. 4(a). It is observed that z_{pr} gradually shifts to the upper region of propagation with an increase in L_B. The value of ω/ω_{ce} at $z = z_{pr}$, which means the magnetic-field strength at the polarization reversal point, is defined as ω/ω_{pr}. This ω/ω_{pr} as a function of L_B is plotted in Fig. 4(b). Since these phenomena are expected to be caused by the effect of the radial boundary, the dependencies of ω/ω_{pr} on L_B are also measured in accordance with changing the plasma radius r_p. The value of ω/ω_{pr} is almost constant with respect to L_B for each plasma radius. These results indicate that the polarization reversal from the LHPW to the RHPW occurs when ω/ω_{ce} attain a certain value. In addition, the value of ω/ω_{pr} is found to become small with an increase in r_p. It is evident that the polarization reversal point is dominated by the plasma radius, i.e., radial boundary condition between the plasma and the vacuum regions.

For an azimuthally symmetric steady-state plasma column, the linear dispersion relation including the effect of radial boundary condition, is referred so as to interpret the observed polarization reversal, and is described as [12]

$$(\gamma^2 + \kappa_2^2 + \gamma k_\perp^2)\kappa_3 + k_\perp^2[\kappa_1(\gamma + k_\perp^2) - \kappa_2^2] = 0, \quad (1)$$
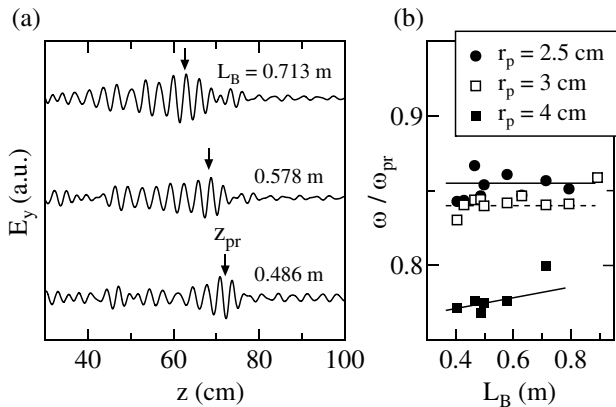
where

$$\frac{\omega^2}{c^2}\mathbf{K} = \begin{pmatrix} \kappa_1 & \kappa_2 & 0 \\ -\kappa_2 & \kappa_1 & 0 \\ 0 & 0 & \kappa_3 \end{pmatrix}, \qquad \gamma = k_\parallel^2 - \kappa_1.$$

Here, $\mathbf{K}$, $k_\parallel$, and $k_\perp$ are dielectric tensor, parallel, and perpendicular wave numbers, respectively. We apply a cold plasma approximation and neglect ion motions in calculating the dispersion relation because of low electron and ion temperatures and $\omega \gg \omega_{pi}, \omega_{ci}$, where $\omega_{pi}/2\pi$ and $\omega_{ci}/2\pi$ are ion plasma and cyclotron frequencies. The experimentally observed radial profile of E_z describes that $m = 0$ mode is formed in our experimental condition and the value of perpendicular wave number is $k_\perp = 1.15$ cm^{-1} at $z = 40$ cm for $r_p = 3$ cm, where $k_\perp$ is generally fixed by the radial boundary condition. In addition, the effects of the inhomogeneous magnetic-field configuration on n_e and $k_\perp$, i.e., the inhomogeneous axial profiles of n_e and $k_\perp$ are taken into account in calculating the dispersion relation with B as a variable. The calculated dispersion relation using the above-mentioned parameters is presented in Fig. 5(a) as a solid line together with the experimental dispersion relations obtained from the LHPW (closed circle) and the RHPW (open square) components, namely, the LW in the high magnetic-field region and the SW growing near the ECR point in Fig. 2(b). The calculated dispersion curve is in good agreement with the
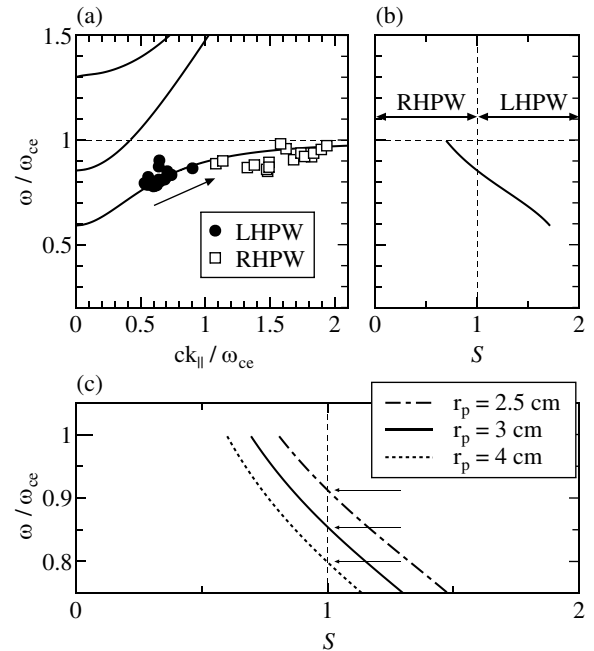

FIG. 4. (a) The RHPW components decomposed from the observed wave patterns for $r_p = 3$ cm and each characteristic length L_B. (b) Dependence of normalized frequency ω/ω_{ce} at the polarization reversal point (ω/ω_{pr}) on L_B for each plasma radius r_p.

FIG. 5. (a) Calculated dispersion relation for the case of $k_\perp = 1.15$ cm^{-1} together with experimental dispersion relations obtained from the LHPW (closed circle) and the RHPW (open square) for $r_p = 3$ cm. (b) Calculated polarization index S corresponding to the dispersion curve agreeing with the experimental dispersion. (c) Calculated polarization index S with r_p as a parameter.

experimental ones. On the other hand, the polarization index S is defined as

$$S \equiv \frac{|E_x + iE_y|}{|E_x - iE_y|}, \qquad (2)$$

where, $0 \leq S < 1$, $S = 1$, and $1 < S \leq \infty$ represent right-handed, linear, and left-handed polarizations, respectively. The polarization index is calculated and plotted in Fig. 5(b) for theoretical verification of the experimentally observed polarization reversal from the LHPW to the RHPW. The value of S is larger than unity in the range of $\omega/\omega_{ce} < 0.85$, namely, the polarization of the wave is left-handed. As the wave approaches the ECR point ($\omega/\omega_{ce} = 1$), the value of S becomes smaller than unity. That is to say, the polarization reversal from the LHPW to the RHPW is theoretically found to occur through a linear polarized wave on the condition of $\omega/\omega_{ce} = 0.85$. Thus, the launched LHPW is efficiently absorbed by ECR, because the polarization of the wave becomes right-handed, obeying the dispersion relation including the effects of the radial boundary, i.e., the perpendicular wave number. Moreover, the polarization index shows the same value at any radial positions in the plasma region for the case of $m = 0$, namely, the polarization reversal simultaneously occurs in the whole cross section of the plasma column. The theoretical expectation is also experimentally confirmed.

In order to clarify the mechanism of the phenomenon that the polarization reversal point changes with an increase in r_p [see Fig. 4(b)], the polarization index is calculated for each plasma radius r_p. The experimentally observed radial profiles of E_z give $k_\perp = 1.2$, 1.15, and 1.1 cm^{-1} for the case of $r_p = 2.5$, 3, and 4 cm, respectively. Therefore, the polarization index S can be calculated for these r_p, that is to say, for these value of $k_\perp$ as presented in Fig. 5(c). The polarization reversal points correspond to ω/ω_{ce} at $S = 1$, i.e., ω/ω_{pr} on the calculated curves, which are expressed as arrows in Fig. 5(c). The calculated ω/ω_{pr} is found to become smaller with an increase in r_p, namely, a decrease in $k_\perp$. The values of ω/ω_{pr} for $r_p = 2.5$, 3, and 4 cm are 0.91, 0.85, and 0.8, respectively, and these values are almost consistent with experimental results observed in Fig. 4(b). Therefore, it is proved that the polarization reversal point from the LHPW to the RHPW is determined by the dispersion relation including the effects of the radial boundary, namely, the perpendicular wave number $k_\perp$.

In conclusion, the propagation and damping mechanisms of the LHPW around ECR frequency are investigated for the case of the inhomogeneously magnetized and coaxially bounded plasma in the conducting vacuum vessel. Our experimental results for the first time demonstrate directly the polarization reversal from the LHPW to the RHPW near the ECR point for the case of azimuthal mode

number $m = 0$. As a result, the anomalous damping of the LHPW, which has been considered not to be related to ECR, is found to occur. The experimentally observed dispersion relation is in good agreement with the calculated one including an effect of the radial boundary, and the polarization index calculated by using the dispersion relation theoretically proves the polarization reversal. Moreover, the effects of the radial boundary, i.e., plasma radius on the polarization reversal, are experimentally and theoretically investigated in detail. These results prove that the perpendicular wave number determined by the radial boundary dominates the polarization reversal point. We believe that the damping region of the electromagnetic wave with ECR frequency can be controlled by externally adjusting the polarization reversal point. This idea could play an important role in the localized electron heating, and so on.

*Electronic address: kazunori@ecei.tohoku.ac.jp

[1] T. Kaneko, R. Hatakeyama, and N. Sato, Phys. Rev. Lett. **80**, 2602 (1998).

[2] K. Yatsu, L. G. Bruskin, T. Cho, M. Hamada, M. Hirata, H. Hojo, M. Ichimura, K. Ishii, A. Itakura, I. Katanuma, Y. Kiwamoto, J. Kohagura, S. Kubota, A. Mase, Y. Nakashima, T. Saito, Y. Sakamoto, T. Tamano, Y. Tatematsu, T. Tokuzawa, and M. Yoshikawa, Nucl. Fusion **39**, 1707 (1999).

[3] D. F. H. Start, N. R. Ainsworth, J. G. Cordey, T. Edlington, W. H. W. Fletcher, M. F. Payne, and T. N. Todd, Phys. Rev. Lett. **48**, 624 (1982).

[4] S. Yoshimura, M. Watanabe, K. Tanabe, A. Nakayama, M. Asakawa, T. Kaehara, M. Nakamura, H. Tanaka, T. Maekawa, and Y. Terumichi, Phys. Plasmas **7**, 276 (2000).

[5] R. D. Tarey, R. K. Jarwal, A. Ganguli, and M. K. Akhtar, Plasma Sources Sci. Technol. **6**, 189 (1997).

[6] Y. Ueda, H. Muta, and Y. Kawai, Appl. Phys. Lett. **74**, 1972 (1999).

[7] G. Lisitano, M. Fontanesi, and S. Bernabei, Phys. Rev. Lett. **26**, 747 (1971).

[8] R. L. Stenzel, Phys. Fluids **19**, 857 (1976).

[9] A. Ganguli, M. K. Akhtar, R. D. Tarey, and R. K. Jarwal, Phys. Lett. A **250**, 137 (1998).

[10] A. Ganguli, M. K. Akhtar, and R. D. Tarey, Phys. Plasmas **5**, 1178 (1998).

[11] T. Kaneko, H. Murai, R. Hatakeyama, and N. Sato, Phys. Plasmas **8**, 1455 (2001).

[12] D. G. Swanson, *Plasma Waves* (Institute of Physics, Bristol and Philadelphia, 2003), 2nd ed., Chap. 5.